Acta Oceanol. Sin., 2020, Vol. 39, No. 9, P. 109–114
https://doi.org/10.1007/s13131-020-1651-8
http://www.hyxb.org.cn
E-mail: hyxbe@263.net

Vertical distribution of nutrient tracers in the western Arctic Ocean and its relationship to water structure and biogeochemical processes

Yanpei Zhuang[1, 2], Hongliang Li[1, 2], Haiyan Jin[1, 3*], Shengquan Gao[1], Jianfang Chen[1, 3*], Yangjie Li[1], Youcheng Bai[1], Zhongqiang Ji[1]

[1] Key Laboratory of Marine Ecosystem Dynamics, Second Institute of Oceanography, Ministry of Natural Resources, Hangzhou 310012, China

[2] Southern Marine Science and Engineering Guangdong Laboratory (Zhuhai), Zhuhai 519080, China

[3] State Key Laboratory of Satellite Ocean Environment Dynamics, Second Institute of Oceanography, Ministry of Natural Resources, Hangzhou 310012, China

Received 20 May 2019; accepted 12 August 2019

Abstract

During the 3rd Chinese National Arctic Research Expedition cruise in the summer of 2008, nutrients (NO_3^-, NO_2^-, SiO_3^{2-}, and PO_4^{3-}) and dissolved oxygen were measured in the western Arctic Ocean, to derive the vertical distribution of nutrient tracers and its relationship to water structure and biogeochemical processes. The nutrient data show that surface waters had the lowest NO_3^-/PO_4^{3-} (mean of 0.5) and SiO_3^{2-}/PO_3^- (mean of 2.8) values in the water column, suggesting an excess of phosphate. Winter Bering Shelf water (wBSW) had high Si* (16.7 μmol/L; Si*=[Si(OH)$_4$]–[NO_3^-]) with negative N* (–11.7 μmol/L; N*=[PO_4^{3-}]–16[PO_4^{3-}]+3.5 μmol/L) in the water column, indicating nitrate deficiency. The warm Atlantic layer had positive N* (0.8 μmol/L) and negative Si* (–5.4 μmol/L) compared with Pacific source water. The vertical distribution of nutrients indicates that wBSW can be characterized by N* minimum and Si* maximum. In contrast, minima of Si* and SiO_3^{2-}/PO_4^{3-} below 200 m indicate the distribution of Atlantic warm water.

Key words: nutrients, N*, Si*, Canada Basin, Arctic Ocean

Citation: Zhuang Yanpei, Li Hongliang, Jin Haiyan, Gao Shengquan, Chen Jianfang, Li Yangjie, Bai Youcheng, Ji Zhongqiang. 2020. Vertical distribution of nutrient tracers in the western Arctic Ocean and its relationship to water structure and biogeochemical processes. Acta Oceanologica Sinica, 39(9): 109–114, doi: 10.1007/s13131-020-1651-8

1 Introduction

The Redfield ratio (i.e., C: N: P=106: 16: 1) is the cornerstone of nutrient dynamics in the ocean (Redfield et al., 1963). On the basis of this ratio, nutrients can be used to trace the origin and transport of water masses, and to assess biogeochemical processes in the water column. Broecker (1974) first proposed quasi-conservative nutrient water mass tracers, NO (NO=[O_2]+9[NO_3^-]) and PO (PO=[O_2]+135[PO_4^{3-}]), which have since been widely used (e.g., Ríos et al., 1989; Ekwurzel et al., 2001; McLaughlin et al., 2004). For example, the NO/PO ratio can be used to discriminate between Pacific (<0.85) and Atlantic (>0.85) waters (Wilson and Wallace, 1990). Gruber and Sarmiento (1997) proposed N*, a parameter for characterizing nitrogen budget processes (N*=([NO_3^-]–16[PO_4^{3-}]+2.90 μmol/kg)×0.87). Deutsch et al. (2001) and Deutsch and Weber (2012) adopted the simplest expression of N* (N*=[NO_3^-]–16[PO_4^{3-}]) to determine the net effect of nitrogen fixation and denitrification (e.g., nitrate excess or loss) relative to phosphate. Deutsch and Weber (2012) found that the N* global mean is close to –3.5 μmol/L; therefore, in this study, we used the formula N*=[NO_3^-]–16[PO_4^{3-}]+3.5 μmol/L. Another widely used nutrient tracer, Si*=[Si(OH)$_4$]–[NO_3^-] (Brzezinski et al., 2002; Sarmiento et al., 2004), indicates nutrient status in response to diatom growth. A positive value of Si* indicates an excess of silicate relative to nitrate.

The western Arctic Ocean has large storage of freshwater (Giles et al., 2012), and its nutrient dynamics are strongly influenced by the Beaufort Gyre (Zhuang et al., 2018). Nutrient tracers have been widely used to explore the contribution of ice-melt, river water, and Pacific water and Atlantic water to the water structure of the western Arctic Ocean. For example, Jones et al. (1998) used N-P correlations to calculate the relative contribution of Pacific water and Atlantic water to the Arctic Ocean. Chen et al. (2003) adopted the end-member model (S-δ^{18}O-PO* and S-δD-SiO_3^{2-}) to investigate halocline formation in the Canada Basin. In addition to the endmember model, combinations of salinity, nutrients, and ^{18}O have also been adopted to estimate the contribution of Pacific water mass to the structure and budget of water in the western Arctic Ocean (e.g., Yamamoto-Kawai et al., 2008; Qi et al., 2017).

Nutrient tracers have proved to be reliable indicators of water mass structure in the western Arctic Ocean (e.g., Jones et al., 1998; Zhuang et al., 2019), although previous studies have fo-

Foundation item: The National Natural Science Foundation of China under contract Nos 41941013, 41776205, 41976226 and 41806228; the Scientific Research Funds of Second Institute of Oceanography, Ministry of Natural Resources, under contract No. QNYC2003; the Chinese Polar Environment Comprehensive Investigation & Assessment Programs under contract Nos 0304 and 0402.
*Corresponding author, E-mail: jinhaiyan@sio.org.cn; jfchen@sio.org.cn

cused primarily on the southern Canada Basin. Sea ice retreat may change the nutrient dynamics in these high-latitude waters, however, information regarding nutrient tracers throughout the western Arctic Ocean is still lacking. In this study, several nutrient tracers (NO_3^-/PO_4^{3-}, SiO_3^{2-}/PO_4^{3-}, NO/PO, N*, and Si*) were used to characterize the water mass in the Canada Basin in order to better understand water structure and biogeochemical processes in the Arctic Ocean basin.

2 Materials and methods

2.1 *Study sites and sampling procedures*

Sampling stations in the Canada Basin and adjacent areas were used for this study as part of the Chinese National Arctic Research Expedition (CHINARE) summer cruise in 2008 (Fig. 1). Seawater samples were collected from 55 stations between 9 August and 6 September using a Rosette sampler and Niskin bottles. Hydrological parameters (e.g., salinity and temperature) were recorded *in situ* using pre-calibrated conductive-temperature-depth sensors (SBE 911 plus; Sea-bird, Bellevue, USA).

2.2 *Nutrient and dissolved oxygen analysis*

Seawater samples were collected at the surface, from various water depths (30 m, 50 m, 75 m, 100 m, 150 m, 200 m, 300 m, 400 m, 500 m, 1 000 m, 2 000 m and 3 000 m), and from the bottom of the basin. Seawater samples were filtered through 0.45 μmol/L acid-cleaned cellulose acetate membranes. Nitrate, phosphate, and silicate were measured onboard using a continuous flow analyzer (Skalar San++, Breda, Netherlands). Nitrite was measured using spectrometric methods. Nutrients were analyzed according to oceanographic specifications (General Administration of Quality Supervision, Inspection and Quarantine of the People's Republic of China and Standardization Administration of China, 2008) and the procedures given by Grasshoff et al. (1999). Analytical precision was ±1% for nitrite, ±2.5% for silicate, and ±2% for nitrate and phosphate. Detection limit was 0.1 μmol/L for silicate and nitrate, and 0.03 μmol/L for phosphate. Dissolved oxygen (DO) was measured by iodometric titration (General Administration of Quality Supervision, Inspection and Quarantine of the People's Republic of China and Standardization Administration of China, 2008) with an analytical precision of ±1%.

3 Results

3.1 *Nutrient vertical profiles*

The vertical distribution of N* shows a gradual decrease from the surface to a minimum at 100 m water depth (Fig. 2a). Between 100 m and 400 m water depth, N* increases markedly, reaching a maximum at 400 m. Values of N* in the deep ocean are more positive compared with those in the upper water column. The maximum and minimum values of N* represent different water masses in which nitrogen processes are significantly different. In contrast, Si* shows no change in surface waters (0–30 m) but gradually increases from 30 m to reach a maximum value at 100 m (Fig. 2b). Below 100 m, Si* declines to reach a minimum at 400 m. Si* remains negative between 400 m and 1 000 m, suggesting depleted silicate relative to nitrate. Below 1 000 m, Si* gradually increases with depth.

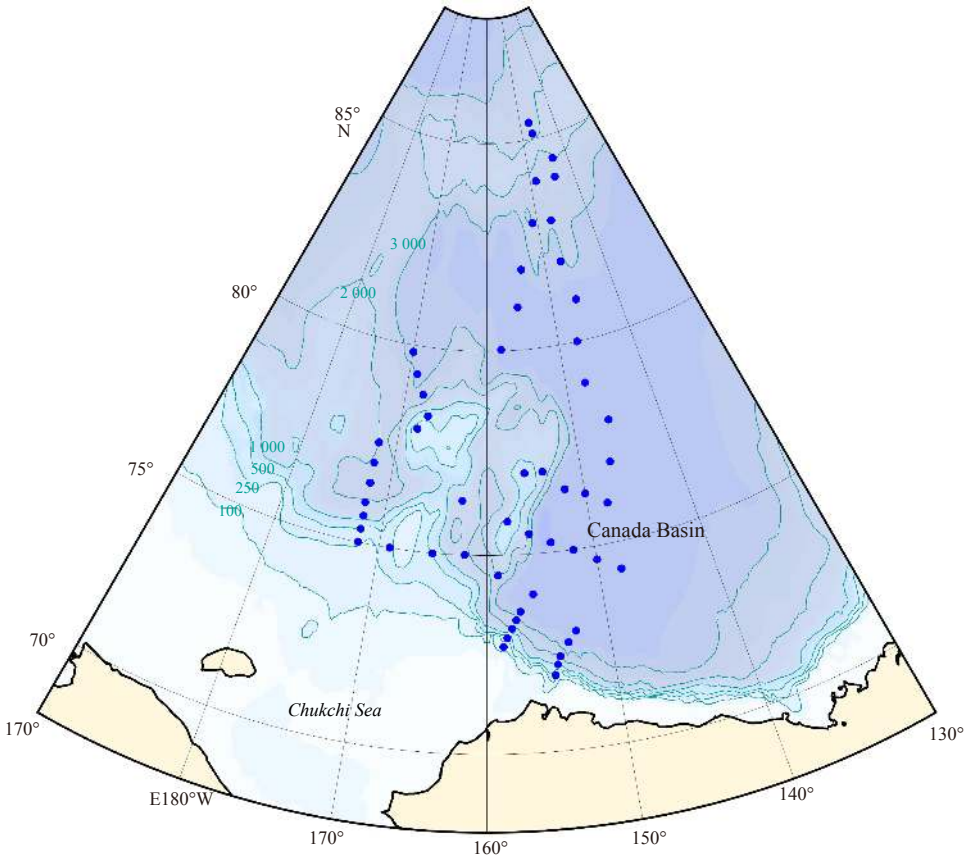

Fig. 1. Sample sites in the western Arctic Ocean during the CHINARE cruise in 2008. Bathymetric lines (water depth in m) from shelf to basin are indicated.

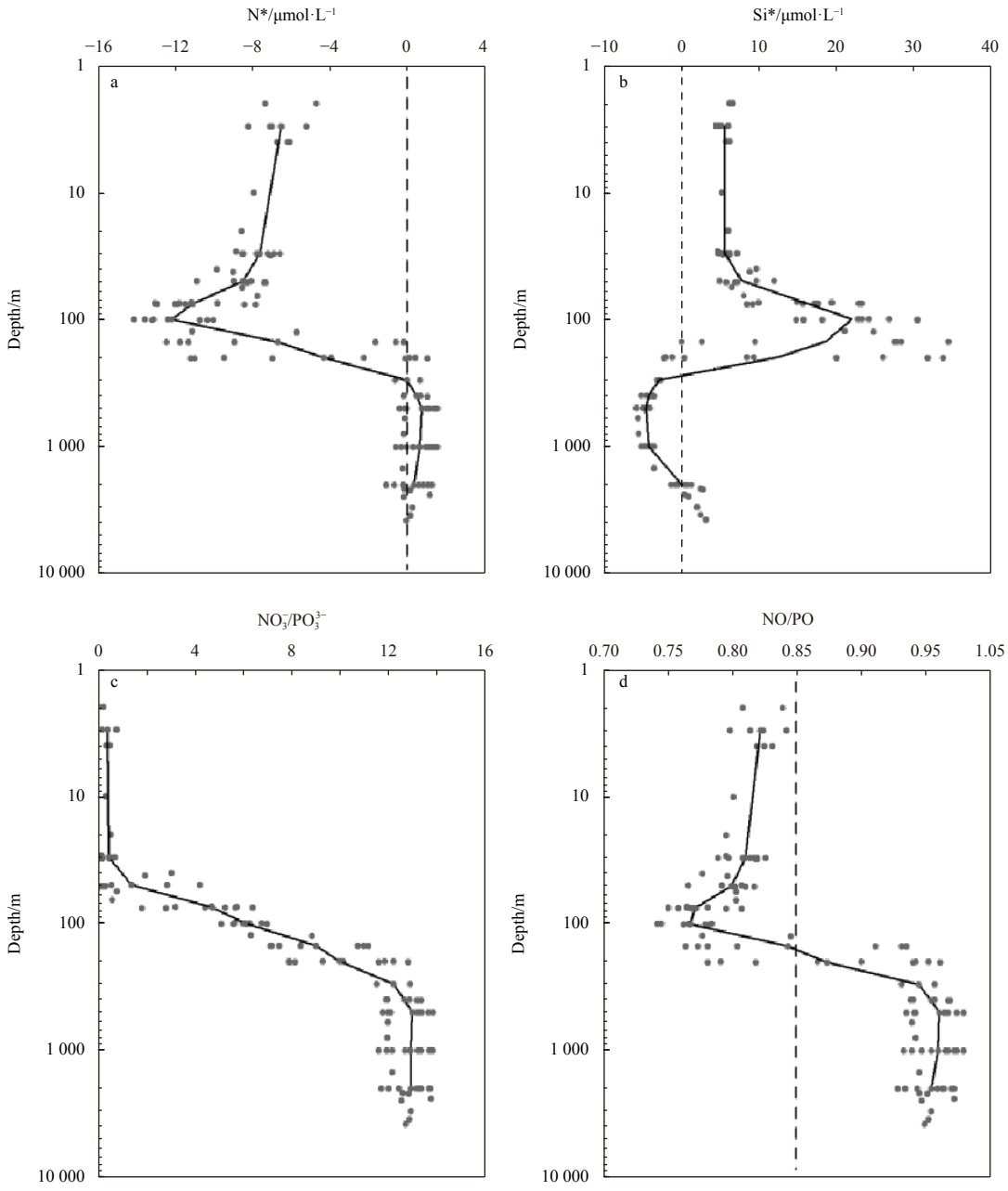

Fig. 2. Vertical profiles in the western Arctic Ocean: N* (a); Si* (b); NO_3^-/PO_4^{3-} (c); and NO/PO (d). Circles represent individual measurements, and the gray line represents mean values with depth. Dashed gray lines represent N*=0, Si*=0 and NO/PO=0.85.

The NO_3^-/PO_4^{3-} ratio shows a linear increase with depth from 30 m to 300 m (Fig. 2c), reflecting the proportional mixing of Pacific water and Atlantic water. The NO_3^-/PO_4^{3-} ratio is relatively stable in surface waters above 30 m (mean of 0.5) and bottom waters deeper than 300 m (mean of 13.1). The vertical distribution of NO/PO is similar to that of NO_3^-/PO_4^{3-} (Fig. 2d). The boundary between Pacific water and Atlantic water can be determined using the NO/PO value of 0.85, which occurs between 150 m and 200 m water depth.

3.2 *Water mass characteristics*

In summer, the surface freshen layer (FL) has a salinity of <31 psu and NO_3^- values of <1 μmol/L and occupies at a depth range of 5–75 m (Fig. 3): this range will vary with ice coverage and freshwater convergence. Halocline water (HW) forms beneath FL and in which salinity gradually increases from 31 psu to 34 psu, although there is little change in temperature (Fig. 3a). The upper halocline (UH) layer consists of Alaska coastal water (ACW) and summer Bering Shelf water (sBSW) (Fig. 3a). Nutrient concentrations in UH water increase with increasing salinity and show a positive correlation between nitrate and phosphate concentrations (Fig. 3b, [N]=11.1, [P]–8, R^2=0.849). The middle halocline (MH) layer is the core of the winter Bering Shelf water (wBSW), which can be defined as a temperature minimum (θ_{min}) and nutrient maximum. The MH layer occurs between water depths of 50 m and 200 m. The wBSW is characterized by cold, saline water with high concentrations of nutrients. MH water has a temperature close to freezing (i.e., down to –1.66°C) and nutrient maxima (PO_4^{3-}>1.4 μmol/L, SiO_3^{2-}>20 μmol/L) (Fig. 3). Atlantic water (AW) originates from the Barents Sea, is transformed

by the Eurasian Shelf and Chukchi Shelf regions, and forms the lower halocline (LH). Below HW is a thermocline layer (HL) where temperatures increase to 0°C. Atlantic Layer (AL) water has high heat capacity (T>0°C) and relatively low phosphate and silicate concentrations compared with Pacific water (Fig. 3). Arctic deep water (ADW) is located at the bottom of the western Arctic Ocean, with a salinity ranging from 34.86 psu to 34.96 psu.

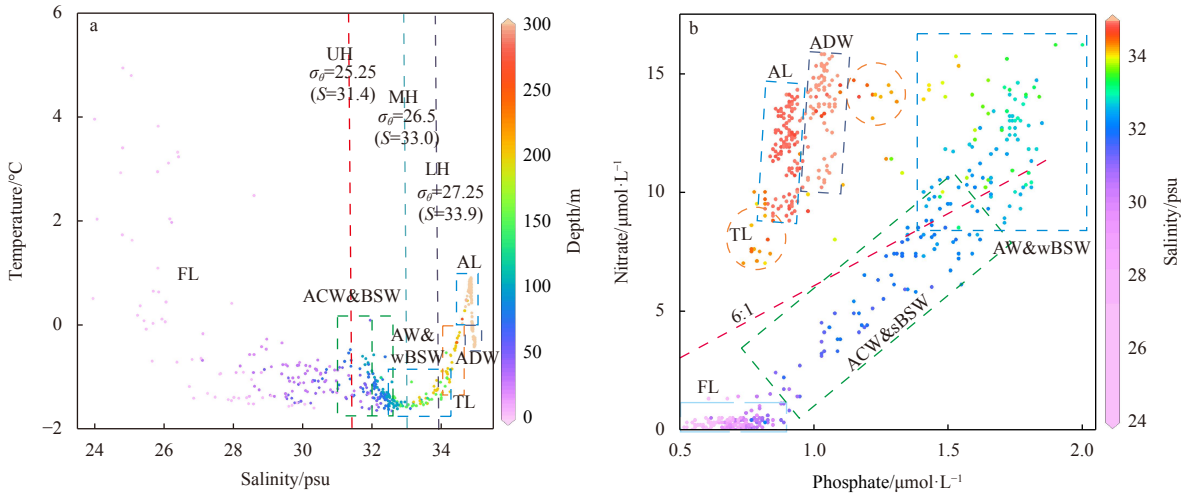

Fig. 3. Temperature-salinity plot for Canada Basin sampling stations, where symbol color represents depth (a); and Nitrate-phosphate plot for Canada Basin sampling stations, where symbol color represents salinity (b). FL (freshen layer), ACW (Alaska coastal water), sBSW (summer Bering Shelf water), wBSW (winter Bering Shelf water), AW (Atlantic water), TL (thermocline layer), AL (Atlantic layer), ADW (Arctic deep water), UH (upper halocline), MH (middle halocline), and LH (lower halocline). UH, MH and LH are based on contours according to McLaughlin et al. (2004) (σ_θ=25.25 kg/m^3 (UH), 26.0 kg/m^3 (MH) and 27.25 kg/m^3 (LH)).

4 Discussion

4.1 *Nutrient tracer signals according to water mass*

To understand and explain the nutrient tracer signals in the western Arctic Ocean, the water column was divided into seven layers on the basis of results of previous studies (e.g., McLaughlin et al., 2004; Steele et al., 2004). The specific characteristics of physical properties and nutrient tracers in the seven water layers are summarized in Table 1.

Layer I (FL) has the lowest nitrate and silicate concentrations in the water column (means of 0.3 μmol/L and 2.1 μmol/L, respectively), as well as the lowest NO_3^-/PO_4^{3-} and SiO_3^{2-}/PO_4^{3-} values (means of 0.5 and 2.8, respectively). These low concentrations represent nitrate limitation for algae growth and an excess of phosphate relative to nitrate and silicate.

ACW and sBSW are the main components of Layer II, which is also known as summer Pacific halocline water (Shimada et al., 2001). The distribution of ACW and sBSW can be distinguished by a temperature maximum under different salinity ranges (Steele et al., 2004; Shi et al., 2005).

The upper boundary of Layer III (wBSW) can be defined using phosphate (PO_4^{3-}>1.4 μmol/L) and silicate (SiO_3^{2-}>

Table 1. Distribution of physical properties and nutrient tracers in the different water layers of the western Arctic Ocean. The water structure is divided into seven layers on the basis of previous studies (e.g., McLaughlin et al., 2004; Steele et al., 2004)

	Layer I	Layer II	Layer III	Layer IV	Layer V	Layer VI	Layer VII
Water mass	FL	ACW, sBSW	wBSW	AW	TL	AL	ADW
Depth/m	5–75	30–100	50–200	125–200	150–250	200–1 000	1 000–3 800
Temperature/°C	–1.60–4.95	–1.64–0.09	–1.66 to –0.62	–1.43 to –0.54	–1.40 to –0.14	0.00–0.90	–0.43 to –0.01
Salinity	23.96–31.15	31.01–32.49	32.02–33.87	33.59–34.26	33.98–34.51	34.59–34.88	34.86–34.96
Density/kg·m^{-3}	19.05–25.03	24.93–26.13	25.75–27.24	27.03–27.54	27.34–27.72	27.77–28.01	28.00–28.09
PO_4^{3-}/μmol·L^{-1}	0.70 ± 0.09	1.26 ± 0.21	1.67 ± 0.12	1.30 ± 0.18	0.88 ± 0.15	0.91 ± 0.05	1.00 ± 0.06
SiO_3^{2-}/μmol·L^{-1}	2.1 ± 1.4	13.6 ± 4.6	28.2 ± 5.3	21.5 ± 5.3	8.4 ± 4.2	6.5 ± 2.1	9.5 ± 2.8
NO_3^-/μmol·L^{-1}	0.3 ± 0.3	6.2 ± 2.5	11.5 ± 2.1	13.0 ± 2.4	9.8 ± 2.4	11.9 ± 1.5	13.0 ± 1.8
NO_2^-/μmol·L^{-1}	0.03 ± 0.03	0.08 ± 0.06	0.05 ± 0.04	0.04 ± 0.04	0.03 ± 0.02	0.04 ± 0.03	0.03 ± 0.02
NO_3^-/PO_4^{3-}	0.5 ± 0.4	4.7 ± 1.5	6.9 ± 1.1	9.9 ± 1.1	11.0 ± 1.3	13.1 ± 1.6	13.1 ± 1.7
SiO_3^{2-}/PO_4^{3-}	2.8 ± 1.6	10.4 ± 2.4	16.8 ± 2.4	16.3 ± 2.4	9.1 ± 2.9	7.0 ± 1.9	9.5 ± 2.3
NO/μmol·L^{-1}	398 ± 15	402 ± 16	412 ± 25	396 ± 20	387 ± 14	407 ± 13	416 ± 15
PO/μmol·L^{-1}	489 ± 24	517 ± 18	534 ± 25	455 ± 25	419 ± 10	423 ± 6	433 ± 5
NO/PO	0.81 ± 0.02	0.78 ± 0.02	0.77 ± 0.03	0.87 ± 0.02	0.93 ± 0.02	0.96 ± 0.03	0.96 ± 0.03
N*/μmol·L^{-1}	–7.4 ± 1.4	–10.5 ± 1.5	–11.7 ± 1.8	–4.3 ± 1.4	–0.8 ± 1.0	0.8 ± 1.4	0.6 ± 1.7
Si*/μmol·L^{-1}	1.7 ± 1.3	7.4 ± 2.5	16.7 ± 4.1	8.5 ± 3.7	–1.3 ± 2.5	–5.4 ± 2.0	–3.5 ± 2.6

Note: FL (freshen layer), ACW (Alaska coastal water), sBSW (summer Bering Shelf water), wBSW (winter Bering Shelf water), AW (Atlantic water), TL (thermocline layer), AL (Atlantic layer), and ADW (Arctic deep water).

20 μmol/L) concentrations (Jin et al., 2004). The lower boundary of Layer III is defined as an NO/PO value of <0.85 (Wilson and Wallace, 1990). Layer III also has the highest concentration of phosphate (mean of 1.67 μmol/L) and silicate (mean of 28.2 μmol/L), constituting a nutrient maximum in the Canada Basin (e.g., Jin et al., 2004). The wBSW has the most negative N* value (mean of –11.7 μmol/L) in the water column, followed by sBSW and ACW (mean of –10.5 μmol/L). These patterns are controlled by strong denitrification in the Bering-Chukchi Shelf (Chang and Devol, 2009).

Layer IV (AW) is characterized by 0.85<NO/PO<0.90 and Si*>4 μmol/L. Layer V is the thermocline layer. Layer VI (AL) has a thickness of ~800 m and originates from the Fram Strait branch (Schauer et al., 1997). The mean values of NO_3^-/PO_4^{3-}, N* and Si* are 13.1, 0.8 μmol/L and –5.4 μmol/L, respectively. The difference in N* (12.5 μmol/L) and Si* (22.1 μmol/L) between AL and wBSW is significant. ADW is located in the bottom of the basin (Layer VII) and has similar N* and NO_3^-/PO_4^{3-} values to those of AL but higher SiO_3^{2-} and SiO_3^{2-}/PO_4^{3-}. The chemical signatures of water masses with multiple sources are different (Jones et al., 2003). The differences in N* and Si* between water layers in the western Arctic Ocean indicate that nutrients can trace and distinguish Pacific water and Atlantic water.

4.2 *Nutrient tracers: implications for biogeochemical processes*

North Atlantic water has the lowest silicate concentration (DeMaster, 1981) and strong nitrogen fixation (e.g., positive N*; Hansell and Follows, 2008) in the global oceans. Therefore, water masses originating from the Atlantic Ocean have positive N*, negative Si*, and high NO_3^-/PO_4^{3-} values (Fig. 4). ADW has a nutrient signature similar to that of Atlantic water, except that it has relatively high SiO_3^{2-} concentrations and SiO_3^{2-}/PO_4^{3-} values, probably as a result of dissolution of biogenic silica in the deep ocean. AW in the lower halocline has a nutrient signature closer to that of a Pacific source rather than an Atlantic source (Fig. 4), as AW originates from the Barents Sea (Jones and Anderson, 1986; Rudels et al., 1996) and is chemically transformed through the broad shelf (McLaughlin et al., 1996).

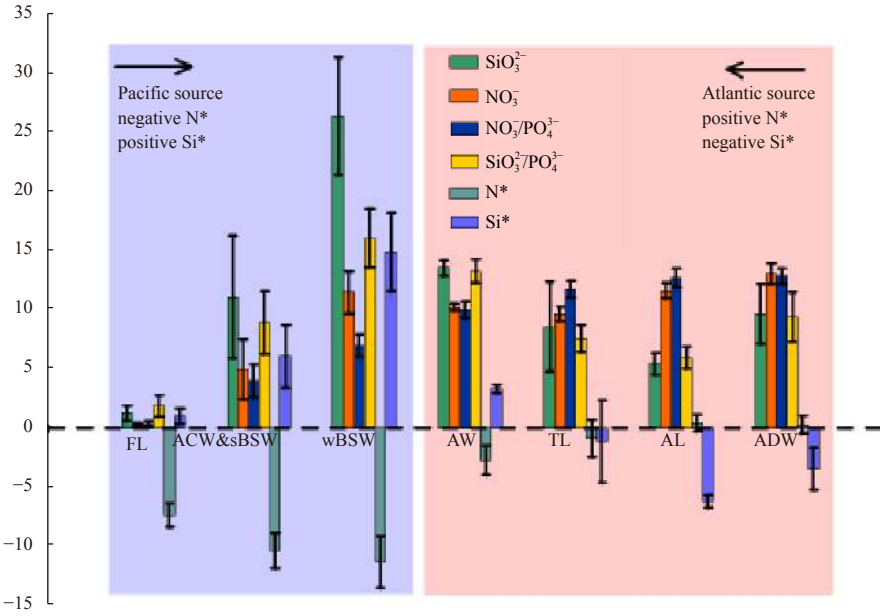

Fig. 4. Nutrient tracer plots for each water mass in the western Arctic Ocean. Abbreviations are as for Fig. 3.

Pacific waters in the western Arctic Ocean include the ACW, sBSW, and wBSW (Zhao et al., 2006), and they dominantly determine the composition of halocline water. The very negative N* values in these waters indicate dominant nitrogen loss relative to phosphate. These patterns are a consequence of Pacific water being originally nitrate deficient (Li et al., 2011), and there is strong denitrification in the Bering-Chukchi Shelf (Chang and Devol, 2009). The Bering-Chukchi Shelf has active biogeochemical cycles and pelagic production under retreating Arctic sea ice (Grebmeier et al., 2010; Li et al., 2017), which enhances the effect of denitrification. The high Si* value of wBSW is due to low biological uptake of silicate in winter. The surface inventory of nitrate in FL is low, resulting in nitrogen limitation and low phytoplankton growth in the western Arctic Ocean.

5 Conclusions

The vertical distribution of nutrient tracers in the western Arctic Ocean indicates that the surface FL has the lowest nitrate and silicate concentrations in the water column (means of 0.3 μmol/L and 2.1 μmol/L, respectively), as well as the lowest NO_3^-/PO_4^{3-} and SiO_3^{2-}/PO_4^{3-} values (means of 0.5 and 2.8, respectively). This causes the FL to be nitrate limited, thus inhibiting algae growth. The wBSW has the highest mean concentration of phosphate [(1.67±0.12) μmol/L] and silicate [(28.2±5.3) μmol/L], with mean values of SiO_3^{2-}/PO_4^{3-}, N* and Si* of 16.8, –11.7 μmol/L and 16.7 μmol/L, respectively. The AL contains positive N* (0.8 μmol/L) and negative Si* (–5.4 μmol/L), in contrast to Pacific water. The ADW shows higher concentrations of SiO_3^{2-} and hence SiO_3^{2-}/PO_4^{3-}, suggesting a contribution by silica recycling. The differences in N* and Si* between Canada Basin water layers indicate that nutrient tracers can distinguish Pacific and Atlantic source waters. The vertical distribution of nutrients indicates that the MH layer can be characterized by N* minimum and Si* maximum. In contrast, Si* minimum and SiO_3^{2-}/PO_4^{3-} values below 200 m indicate the distribution of Atlantic warm water.

Acknowledegements

We thank the crew members of the *Xuelong* icebreaker during Chinese Arctic Expeditions. CTD data were provided by Jinping Zhao from the Ocean University of China and issued

through a polar scientific data sharing platform maintained by the Chinese National Arctic and Antarctic Data Center (CNAADC: (http://www.chinare.org.cn). Thanks are also given to Zhengbing Han from the Second Institute of Oceanography for help with fieldwork.

References

Broecker W S. 1974. "NO", a conservative water-mass tracer. Earth and Planetary Science Letters, 23(1): 100–107, doi: 10.1016/0012-821X(74)90036-3

Brzezinski M A, Pride C J, Franck V M, et al. 2002. A switch from $Si(OH)_4$ to NO_3^- depletion in the glacial Southern Ocean. Geophysical Research Letters, 29(12): 1564, doi: 10.1029/2001GL014349

Chang B X, Devol A H. 2009. Seasonal and spatial patterns of sedimentary denitrification rates in the Chukchi Sea. Deep Sea Research Part II: Topical Studies in Oceanography, 56(17): 1339–1350, doi: 10.1016/j.dsr2.2008.10.024

Chen Min, Huang Yipu, Jin Mingming, et al. 2003. The sources of the upper and lower halocline water in the Canada Basin derived from isotopic tracers. Science in China Series D: Earth Sciences, 46(6): 625–639, doi: 10.1007/BF02984540

DeMaster D J. 1981. The supply and accumulation of silica in the marine environment. Geochimica et Cosmochimica Acta, 45(10): 1715–1732, doi: 10.1016/0016-7037(81)90006-5

Deutsch C, Gruber N, Key R M, et al. 2001. Denitrification and N_2 fixation in the Pacific Ocean. Global Biogeochemical Cycles, 15(2): 483–506, doi: 10.1029/2000GB001291

Deutsch C, Weber T. 2012. Nutrient ratios as a tracer and driver of ocean biogeochemistry. Annual Review of Marine Science, 4: 113–141, doi: 10.1146/annurev-marine-120709-142821

Ekwurzel B, Schlosser P, Mortlock R A, et al. 2001. River runoff, sea ice meltwater, and Pacific water distribution and mean residence times in the Arctic Ocean. Journal of Geophysical Research: Oceans, 106(C5): 9075–9092, doi: 10.1029/1999JC000024

General Administration of Quality Supervision, Inspection and Quarantine of the People's Republic of China, Standardization Administration of China. 2008. GB/T 12763-2007 Specifications for oceanographic survey (in Chinese). Beijing: China Standard Press

Giles K A, Laxon S W, Ridout A L, et al. 2012. Western Arctic Ocean freshwater storage increased by wind-driven spin-up of the Beaufort Gyre. Nature Geoscience, 5(3): 194–197, doi: 10.1038/ngeo1379

Grasshoff K, Kremling K, Ehrhardt M. 1999. Methods of Seawater Analysis. Weinheim: Wiley-VCH, 193–198

Grebmeier J M, Moore S E, Overland J E, et al. 2010. Biological response to recent pacific Arctic sea ice retreats. Eos, Transactions American Geophysical Union, 91(18): 161–162, doi: 10.1029/2010EO180001

Gruber N, Sarmiento J L. 1997. Global patterns of marine nitrogen fixation and denitrification. Global Biogeochemical Cycles, 11(2): 235–266, doi: 10.1029/97GB00077

Hansell D A, Follows M J. 2008. Nitrogen in the Atlantic Ocean. In: Capone D G, Bronk D A, Mulholland M R, et al., eds. Nitrogen in the Marine Environment. 2nd ed. Oxford: Elsevier, 597–630

Jin Mingming, Wu Jingfeng, Chen Jianfang, et al. 2004. Nutrient maximum in the Canada Basin. Chinese Journal of Polar Research (in Chinese), 16(3): 240–252

Jones E P, Anderson L G. 1986. On the origin of the chemical properties of the Arctic Ocean halocline. Journal of Geophysical Research: Oceans, 91(C9): 10759–10767, doi: 10.1029/JC091iC09p10759

Jones E P, Anderson L G, Swift J H. 1998. Distribution of Atlantic and Pacific waters in the upper Arctic Ocean: implications for circulation. Geophysical Research Letters, 25(6): 765–768, doi: 10.1029/98GL00464

Jones E P, Swift J H, Anderson L G, et al. 2003. Tracing Pacific water in the North Atlantic Ocean. Journal of Geophysical Research: Oceans, 108(C4): 3116, doi: 10.1029/2001JC001141

Li Hongliang, Chen Jianfang, Gao Shengquan, et al. 2011. Nutrients variation of the Pacific inflow in the western Arctic Ocean. Haiyang Xuebao (in Chinese), 33(2): 85–95, doi: 10.1029/2001JC001141

Li Chengxuan, Wang Baodong, Yang Guipeng, et al. 2017. Occurrence and turnover of biogenic sulfur in the Bering Sea during summer. Journal of Geophysical Research: Oceans, 122(11): 8567–8592, doi: 10.1002/2017JC013299

McLaughlin F A, Carmack E C, Macdonald R W, et al. 1996. Physical and geochemical properties across the Atlantic/Pacific water mass front in the southern Canadian Basin. Journal of Geophysical Research: Oceans, 101(C1): 1183–1197, doi: 10.1029/95JC02634

McLaughlin F A, Carmack E C, Macdonald R W, et al. 2004. The joint roles of Pacific and Atlantic-origin waters in the Canada Basin, 1997–1998. Deep Sea Research Part I: Oceanographic Research Papers, 51(1): 107–128, doi: 10.1016/j.dsr.2003.09.010

Qi Di, Chen Liqi, Chen Baoshan, et al. 2017. Increase in acidifying water in the western Arctic Ocean. Nature Climate Change, 7(3): 195–199, doi: 10.1038/nclimate3228

Redfield A C, Ketchum B H, Richards F A. 1963. The influence of organisms on the composition of the sea water. In: Hill M N, ed. The Sea. New York: Interscience, 26–77

Ríos A F, Fraga F, Pérez F F. 1989. Estimation of coefficients for the calculation of "NO", "PO" and "CO", starting from the elemental composition of natural phytoplankton. Scientia Marina, 53(4): 779–784

Rudels B, Anderson L G, Jones E P. 1996. Formation and evolution of the surface mixed layer and halocline of the Arctic Ocean. Journal of Geophysical Research: Oceans, 101(C4): 8807–8821, doi: 10.1029/96JC00143

Sarmiento J L, Gruber N, Brzezinski M A, et al. 2004. High-latitude controls of thermocline nutrients and low latitude biological productivity. Nature, 427(6969): 56–60, doi: 10.1038/nature02127

Schauer U, Muench R D, Rudels B, et al. 1997. Impact of eastern Arctic shelf waters on the Nansen Basin intermediate layers. Journal of Geophysical Research: Oceans, 102(C2): 3371–3382, doi: 10.1029/96JC03366

Shi Jiuxin, Cao Yong, Zhao Jinping, et al. 2005. Distribution of Pacific-origin water in the region of the Chukchi Plateau in the Arctic Ocean in the summer of 2003. Acta Oceanologica Sinica, 24(6): 12–24

Shimada K, Carmack E C, Hatakeyama K, et al. 2001. Varieties of shallow temperature maximum waters in the western Canadian Basin of the Arctic Ocean. Geophysical Research Letters, 28(18): 3441–3444, doi: 10.1029/2001GL013168

Steele M, Morison J, Ermold W, et al. 2004. Circulation of summer Pacific halocline water in the Arctic Ocean. Journal of Geophysical Research: Oceans, 109(C2): C02027, doi: 10.1029/2003JC002009

Wilson C, Wallace D W R. 1990. Using the nutrient ratio NO/PO as a tracer of continental shelf waters in the central Arctic Ocean. Journal of Geophysical Research: Oceans, 95(C12): 22193–22208, doi: 10.1029/JC095iC12p22193

Yamamoto-Kawai M, McLaughlin F A, Carmack E C, et al. 2008. Freshwater budget of the Canada Basin, Arctic Ocean, from salinity, $\delta^{18}O$, and nutrients. Journal of Geophysical Research: Oceans, 113(C1): C01007, doi: 10.1029/2006JC003858

Zhao Jinping, Shi Jiuxin, Gao Guoping, et al. 2006. Water mass of the northward throughflow in the Bering Strait in the summer of 2003. Acta Oceanologica Sinica, 25(2): 25–32

Zhuang Yanpei, Jin Haiyan, Chen Jianfang, et al. 2018. Nutrient and phytoplankton dynamics driven by the Beaufort Gyre in the western Arctic Ocean during the period 2008–2014. Deep Sea Research Part I: Oceanographic Research Papers, 137: 30–37, doi: 10.1016/j.dsr.2018.05.002

Zhuang Yanpei, Li Hongliang, Jin Haiyan, et al. 2019. Observation of nitrate deficit along transects across the Canada Basin after major sea-ice loss. Polar Science, 21: 224–227, doi: 10.1016/j.polar.2019.03.001